

# Lee-Yang theory of the superradiant phase transition in the open Dicke model

Fredrik Brange,<sup>1</sup> Neill Lambert,<sup>2,3</sup> Franco Nori,<sup>2,3,4</sup> and Christian Flindt<sup>1,3</sup>

<sup>1</sup>*Department of Applied Physics, Aalto University, 00076 Aalto, Finland*

<sup>2</sup>*Theoretical Quantum Physics Laboratory, Cluster for Pioneering Research, RIKEN, Wakoshi, Saitama 351-0198, Japan*

<sup>3</sup>*RIKEN Center for Quantum Computing, Wakoshi, Saitama 351-0198, Japan*

<sup>4</sup>*Physics Department, University of Michigan, Ann Arbor, MI 48109-1040, USA*

The Dicke model describes an ensemble of two-level atoms that are coupled to a confined light mode of an optical cavity. Above a critical coupling, the cavity becomes macroscopically occupied, and the system enters the superradiant phase. This phase transition can be observed by detecting the photons that are emitted from the cavity; however, it only becomes apparent in the limit of long observation times, while actual experiments are of a finite duration. To circumvent this problem, we here make use of recent advances in Lee-Yang theories of phase transitions to show that the superradiant phase transition can be inferred from the factorial cumulants of the photon emission statistics obtained during a finite measurement time. Specifically, from the factorial cumulants, we can determine the complex singularities of generating functions that describe the photon emission statistics, and by extrapolating their positions to the long-time limit, one can detect the superradiant phase transition. We also show that the convergence points determine the tails of the large-deviation statistics of the photon current. Our work demonstrates how phase transitions in the Dicke model and in other quantum many-body systems can be detected from measurements of a finite duration.

## I. INTRODUCTION

The Dicke model, or the Dicke-Hepp-Lieb model, describes a quantum many-body system that exhibits a superradiant phase transition at a critical light-matter coupling [1–4]. It consists of a large ensemble of two-level atoms that interact with a single light-mode of an optical cavity, as illustrated in Fig. 1(a). It can also be realized using superconducting circuits [5–14], trapped ions [15], or collective electronic systems [16]. Above the critical coupling, the system enters the superradiant phase, where the ground state acquires a macroscopic cavity occupation with the photon number being on the order of the number of atoms. Because of its simplicity, the model has been used to investigate a range of critical phenomena, including chaos [17, 18] and entanglement [19] at criticality. Still, a direct experimental observation of the superradiant phase transition has proven challenging [4].

To observe the superradiant phase transition, effective physical realizations involving driven-dissipative systems have been explored. In these setups, internal [20, 21] or motional [22, 23] degrees of freedom are pumped to realize effective strong couplings, but with finite dissipation rates. The combination of the external driving and dissipation results in a non-equilibrium phase transition, which is of a different universality class than for the closed system [4, 20, 24]. However, this phase transition is easier to access experimentally, and it will be the focus of our work. The phase transition occurs in the thermodynamic limit of many atoms and is visible in the photon emission statistics collected over a long time. For example, the cavity occupation changes abruptly at the critical coupling [25]. At the same, however, measurements of the photon counting statistics are of a finite duration, so practical approaches to predict the long-time behavior from finite-time statistics are called for.

In this work, we make use of recent advances in Lee-

Yang theories of phase transitions to observe the superradiant phase transition in the open Dicke model from the photon counting statistics measured during a finite observation time. The theory of phase transitions by Lee and Yang was originally formulated for equilibrium

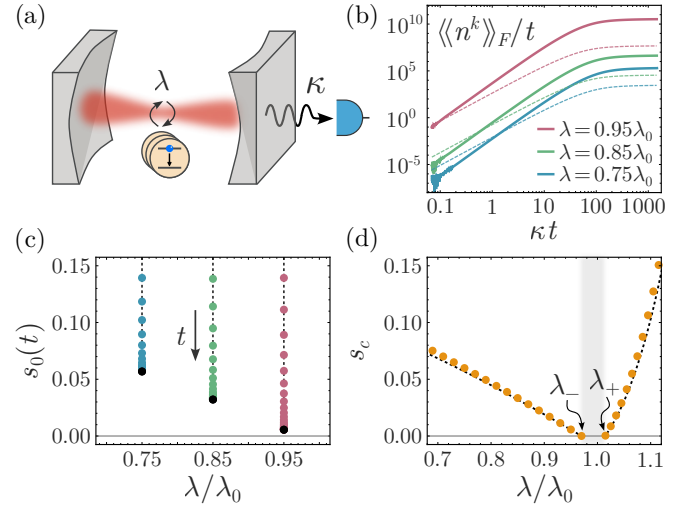


FIG. 1. Lee-Yang theory of the open Dicke model. (a) The system consists of an optical cavity with resonance frequency  $\omega_c$  that is coupled to  $N$  two-level atoms with energy splitting  $\hbar\omega_a$ . The coupling amplitude is denoted by  $\lambda$ , while  $\kappa$  is the rate at which photons are emitted from the cavity. (b) Fourth (dashed,  $k = 4$ ) and fifth (solid,  $k = 5$ ) factorial cumulant of the photon emission statistics in the normal phase. (c) Poles of the factorial cumulant generating function extracted from the results in panel (b). The black dots mark the convergence points in the long-time limit. (d) Extracted convergence points as a function of the coupling. Parameters are  $\omega_c = 2\kappa$  and  $\omega_a = 0.5\kappa$ , and  $\lambda_0$  denotes the critical point of the closed Dicke model, while  $\lambda_-$  and  $\lambda_+$  are the critical points of the open Dicke model according to Eqs. (12, 22).

phase transitions [26–29]. It concerns the zeros of the partition function in the complex plane of a control parameter, for example, the inverse temperature or an external magnetic field. For systems of finite size, the zeros are complex. However, if the system exhibits a phase transition, the zeros will move towards the critical point on the real axis as the thermodynamic limit is approached. The theory of Lee and Yang has been extended to other types of phase transitions, including non-equilibrium phase transitions [28–30], trajectory phase transitions [31], dynamical quantum phase transitions [32–35], and quantum phase transitions at zero temperature [36–38]. Lee-Yang zeros have also been determined in several experiments [39–42].

In the approach we follow here, the phase transition is inferred from the photon counting statistics collected during a finite observation time [31, 41]. As illustrated in Fig. 1(b), we use the high factorial cumulants of the photon counting statistics to extract the dominant pole of the corresponding generating function, which plays the role of the partition function for equilibrium systems. As shown in Fig. 1(c), we can then determine the convergence point in the limit of long observation times. Away from the phase transition, the convergence point is non-zero. However, as we tune the coupling to its critical value, the dominant pole converges to zero, and we can detect the phase transition, as illustrated in Fig. 1(d).

The rest of our article is organized as follows. In Sec. II, we derive a master equation for the open Dicke model in the limit of many atoms. Here, we follow earlier works on the Dicke model, and we include this section for the sake of completeness. In Sec. III, we consider the photon emission statistics from the cavity and derive an analytic expression for the generating function, which is valid at all times. In Sec. IV, we describe the Lee-Yang theory to detect the superradiant phase transition from the photon counting statistics measured during a finite observation time. In Sec. V, we use this approach to determine the critical behavior of the open Dicke model from the high factorial cumulants of the photon counting statistics. We also show how the extracted convergence points control the tails of the large-deviation statistics of the photon current. Finally, in Sec. VI, we conclude on our work and provide an outlook on possible developments for the future. A few technical details are deferred to App. A.

## II. DICKE MODEL

Figure 1(a) shows a physical implementation of the Dicke model consisting of a single-mode optical cavity coupled to an ensemble of two-level atoms. Other realizations include superconducting circuits [5–14], trapped ions [15], and collective electronic systems [16]. Some implementations have been based on driving internal transitions of multi-level atoms [20, 21], or on the motional states of atoms in a Bose-Einstein condensate [22, 23]. The latter implementation involves dissipative effects,

which we will also include in our treatment.

We denote the frequency of the cavity by  $\omega_c$ , while  $\omega_a$  determines the energy splitting of the two-level atoms. The Hamiltonian of the cavity-atom system reads

$$\hat{H} = \hbar\omega_c \hat{c}^\dagger \hat{c} + \hbar\omega_a \hat{J}_z + \frac{\hbar\lambda}{\sqrt{N}} (\hat{c}^\dagger + \hat{c}) (\hat{J}_+ + \hat{J}_-), \quad (1)$$

where  $N$  is the number of atoms, and  $\lambda$  denotes the coupling between the cavity and the atoms. We have also introduced the creation and annihilation operators of the cavity,  $\hat{c}^\dagger$  and  $\hat{c}$ . We treat the ensemble of two-level atoms as a pseudo-spin of length  $N/2$ , and  $\hat{J}_z$  and  $\hat{J}_\pm$  are then collective angular momentum operators with  $\hat{J}_z$  measuring the angular momentum in the  $z$ -direction, while  $\hat{J}_\pm$  are the usual raising and lowering operators.

As illustrated in Fig. 1(a), photons are emitted from the cavity at the rate  $\kappa$ . Correspondingly, the density matrix of the open cavity-atom system evolves according to the Lindblad equation

$$\frac{d}{dt} \hat{\rho}(t) = -\frac{i}{\hbar} [\hat{H}, \hat{\rho}(t)] + \kappa \mathcal{D}[\hat{c}] \hat{\rho}(t), \quad (2)$$

where the commutator accounts for the unitary dynamics of the system if isolated. The dissipator

$$\mathcal{D}[\hat{c}] \hat{\rho}(t) = \hat{c} \hat{\rho}(t) \hat{c}^\dagger - \frac{1}{2} \{ \hat{c}^\dagger \hat{c}, \hat{\rho}(t) \} \quad (3)$$

describes the emission of photons from the cavity. Related to the realizations discussed in Refs. [20, 22], the cavity and atomic frequencies in Eq. (1) are effective frequencies in a rotating frame of a drive, and the dissipation in Eq. (2) acts locally on the cavity mode only. In that respect, it is a non-equilibrium problem as the dissipation will not cool the system to its ground state, but instead it will lead to a non-equilibrium steady-state.

We now derive an effective model in the thermodynamic limit of many atoms. To this end, we follow Refs. [18, 43] and repeat the main steps for the sake of completeness. First, we employ a Holstein-Primakoff transformation [44, 45] to represent the many atoms by a single bosonic mode. Specifically, we express the angular momentum operators in terms of bosonic operators as

$$\begin{aligned} \hat{J}_+ &= \hat{a}^\dagger \sqrt{N - \hat{a}^\dagger \hat{a}}, \\ \hat{J}_- &= \sqrt{N - \hat{a}^\dagger \hat{a}} \hat{a}, \end{aligned} \quad (4)$$

and

$$\hat{J}_z = \hat{a}^\dagger \hat{a} - N/2 \quad (5)$$

where the creation and annihilation operators fulfill the usual bosonic commutation relation  $[\hat{a}, \hat{a}^\dagger] = 1$ . Under this transformation, the Hamiltonian becomes

$$\begin{aligned} \hat{H} &= \hbar\omega_c \hat{c}^\dagger \hat{c} + \hbar\omega_a \hat{a}^\dagger \hat{a} \\ &+ \hbar\lambda (\hat{c}^\dagger + \hat{c}) \left( \hat{a}^\dagger \sqrt{1 - \frac{\hat{a}^\dagger \hat{a}}{N}} + \sqrt{1 - \frac{\hat{a}^\dagger \hat{a}}{N}} \hat{a} \right), \end{aligned} \quad (6)$$

having omitted an offset that is proportional to  $N$ .

We now consider the thermodynamic limit. For small couplings, the system is in the normal phase, where averages of  $\hat{a}^\dagger \hat{a}$  do not grow with  $N$ , and we obtain

$$\hat{H}_{\text{NP}} = \hbar\omega_c \hat{c}^\dagger \hat{c} + \hbar\omega_a \hat{a}^\dagger \hat{a} + \hbar\lambda (\hat{c}^\dagger + \hat{c}) (\hat{a}^\dagger + \hat{a}). \quad (7)$$

The dissipator in Eq. (2) is independent of the number of atoms. Therefore, the Lindblad equation becomes

$$\frac{d}{dt} \hat{\rho}(t) = -\frac{i}{\hbar} [\hat{H}_{\text{NP}}, \hat{\rho}(t)] + \kappa \mathcal{D}[\hat{c}] \hat{\rho}(t). \quad (8)$$

Next, we diagonalize the Hamiltonian using eigenvalue decompositions such that

$$\hat{c} = \varepsilon_{1-} \hat{d}_1 + \varepsilon_{1+} \hat{d}_1^\dagger + \varepsilon_{2-} \hat{d}_2 + \varepsilon_{2+} \hat{d}_2^\dagger \quad (9)$$

with a similar expression for the operator  $\hat{a}$ , which eventually drops out. The Hamiltonian then becomes

$$\hat{H}_D = \hbar\omega_1 \hat{d}_1^\dagger \hat{d}_1 + \hbar\omega_2 \hat{d}_2^\dagger \hat{d}_2 \quad (10)$$

with the corresponding master equation reading

$$\begin{aligned} \frac{d}{dt} \hat{\rho}(t) = & -\frac{i}{\hbar} [\hat{H}_D, \hat{\rho}(t)] \\ & + \kappa \left( \varepsilon_{1-}^2 \mathcal{D}[\hat{d}_1] + \varepsilon_{1+}^2 \mathcal{D}[\hat{d}_1^\dagger] + \varepsilon_{2-}^2 \mathcal{D}[\hat{d}_2] + \varepsilon_{2+}^2 \mathcal{D}[\hat{d}_2^\dagger] \right) \hat{\rho}(t), \end{aligned} \quad (11)$$

having omitted fast-rotating terms of the form  $\hat{d}_1^\dagger \hat{d}_2^\dagger$ . The coefficients  $\varepsilon_{1\pm, 2\pm}$  and the frequencies  $\omega_{1,2}$  are defined in App. A. The smallest frequency vanishes if

$$\lambda_- = \frac{\sqrt{\omega_c \omega_a}}{2}, \quad (12)$$

which sets an upper limit on  $\lambda$  for the normal phase.

In the superradiant phase, the average occupation of the cavity and the number of excited atoms increase with  $N$ . We thus employ a mean-field ansatz to find an effective Hamiltonian in the thermodynamic limit. To this end, we define the operators

$$\check{c} = \hat{c} - \sqrt{r_c N}, \quad \check{a} = \hat{a} + \sqrt{r_a N}, \quad (13)$$

which are independent of  $N$ , and  $r_a$  is a real constant, while  $r_c$  can be complex. The macroscopic occupation is determined such that all terms proportional to  $\sqrt{N}$  vanish in the master equation, yielding the condition for a stable stationary state that [18, 43]

$$r_c = \frac{4\lambda^2 \left[ 1 - (\lambda_0/\lambda)^4 \right]}{(2\omega_c - i\kappa)^2}, \quad (14)$$

and

$$r_a = [1 - (\lambda_0/\lambda)^2]/2. \quad (15)$$

Here, we have defined the coupling

$$\lambda_0 = \sqrt{(\kappa^2 + 4\omega_c^2)\omega_a/16\omega_c}, \quad (16)$$

above which occupations become macroscopic in the limiting case of vanishing emission rate,  $\kappa = 0$ .

The Hamiltonian in the superradiant phase now reads

$$\begin{aligned} \hat{H}_{\text{SP}} = & \hbar\omega_c \check{c}^\dagger \check{c} + \hbar\Omega_a \check{a}^\dagger \check{a} + \hbar\lambda_{\text{aa}} (\check{a}^\dagger + \check{a})^2 \\ & + \hbar\lambda_{\text{ca}} (\check{c}^\dagger + \check{c}) (\check{a}^\dagger + \check{a}), \end{aligned} \quad (17)$$

where we have introduced the frequency

$$\Omega_a = \omega_a + \lambda\sqrt{N} \frac{2r_a}{\sqrt{1-r_a}} \text{Re}\{\sqrt{r_c}\}, \quad (18)$$

together with the couplings

$$\lambda_{\text{ca}} = \lambda \frac{1-2r_a}{\sqrt{1-r_a}}, \quad (19)$$

and

$$\lambda_{\text{aa}} = \lambda \frac{(2-r_a)\sqrt{r_a}}{2(1-r_a)^{3/2}} \text{Re}\{\sqrt{r_c}\}. \quad (20)$$

Moreover, the master equation becomes

$$\frac{d}{dt} \hat{\rho}(t) = -\frac{i}{\hbar} [\hat{H}_{\text{SP}}, \hat{\rho}(t)] + \kappa \mathcal{D}[\check{c}] \hat{\rho}(t). \quad (21)$$

Just as in the normal phase, we can diagonalize the Hamiltonian using eigenvalue decompositions. We then arrive at the same Hamiltonian and master equation as in Eqs. (10) and (11), however, with different coefficients  $\varepsilon_{1\pm, 2\pm}$  and frequencies  $\omega_{1,2}$  as detailed in App. A. In this case, the smallest frequency vanishes for

$$\lambda_+ = \frac{(\kappa^2 + 4\omega_c^2)^{3/4} \sqrt{\omega_a}}{4\sqrt{2}\omega_c}, \quad (22)$$

which sets a lower limit on  $\lambda$  for the superradiant phase. We note that  $\lambda_+$  depends on  $\kappa$ , and only when  $\kappa \ll \omega_c$ , we have  $\lambda_+ = \lambda_-$ . It will also be important that the master equation in Eq. (11) describes two uncoupled quantum harmonic oscillators.

### III. PHOTON EMISSION STATISTICS

To observe the phase transitions using our Lee-Yang theory, we consider the probability  $P(n, t)$  that  $n$  photons are emitted during the time span  $[0, t]$ . It is useful to introduce the factorial moment generating function

$$\mathcal{M}_F(s, t) = \sum_{n=0}^{\infty} P(n, t) (1+s)^n, \quad (23)$$

which yields the factorial moments upon differentiation with respect to the counting variable  $s$  as

$$\langle n^k \rangle_F(t) = \partial_s^k \mathcal{M}_F(s, t) \Big|_{s=0}. \quad (24)$$

The factorial moments are given by the ordinary ones as

$$\langle n^k \rangle_F = \langle n(n-1)\dots(n-k+1) \rangle. \quad (25)$$

For instance, the first two factorial moments read  $\langle n \rangle_F = \langle n \rangle$  and  $\langle n^2 \rangle_F = \langle n^2 \rangle - \langle n \rangle$  in terms of the ordinary ones. We also define the factorial cumulant generating function

$$\mathcal{F}_F(s, t) = \ln \mathcal{M}_F(s, t), \quad (26)$$

which yields the factorial cumulants as

$$\langle\langle n^k \rangle\rangle_F(t) = \partial_s^k \mathcal{F}_F(s, t)|_{s=0}. \quad (27)$$

The factorial cumulants can also be expressed in terms of the ordinary ones as

$$\langle\langle n^k \rangle\rangle_F = \langle\langle n(n-1)\dots(n-k+1) \rangle\rangle. \quad (28)$$

Factorial cumulants are useful to characterize discrete quantities, such as the number of photons [46–50]. Indeed, for a Poisson distribution, only the first factorial cumulant is non-zero. By contrast, ordinary cumulants are useful to characterize continuous variables, and they are defined so that only the first two cumulants are non-zero for a Gaussian distribution.

To find the generating functions, we resolve the density matrix with respect to the number of emitted photons during the time span  $[0, t]$ , which defines  $\hat{\rho}(n, t)$  [51]. We can then express the photon counting statistics as

$$P(n, t) = \text{tr} \{ \hat{\rho}(n, t) \}. \quad (29)$$

These density matrices obey the system of equations

$$\begin{aligned} \frac{d}{dt} \hat{\rho}(n, t) = & -\frac{i}{\hbar} \left[ \hat{H}, \hat{\rho}(n, t) \right] \\ & + \kappa \left( \hat{c} \hat{\rho}(n-1, t) \hat{c}^\dagger - \frac{1}{2} \{ \hat{c}^\dagger \hat{c}, \hat{\rho}(n, t) \} \right). \end{aligned} \quad (30)$$

To solve these coupled equations, we define

$$\hat{\rho}(s, t) = \sum_{n=0}^{\infty} \hat{\rho}(n, t) (1+s)^n, \quad (31)$$

whose equation of motions reads

$$\frac{d}{dt} \hat{\rho}(s, t) = -\frac{i}{\hbar} \left[ \hat{H}, \hat{\rho}(s, t) \right] + \kappa \mathcal{D}_s[\hat{c}] \hat{\rho}(s, t), \quad (32)$$

where the counting variable now enters the dissipator as

$$\mathcal{D}_s[\hat{c}] \hat{\rho} = (1+s) \hat{c} \hat{\rho} \hat{c}^\dagger - \frac{1}{2} \{ \hat{c}^\dagger \hat{c}, \hat{\rho} \}. \quad (33)$$

Solving for  $\rho(s, t)$ , we obtain the generating function as

$$\mathcal{M}_F(s, t) = \text{tr} \{ \hat{\rho}(s, t) \}. \quad (34)$$

Next, we employ the diagonalization in Eq. (9) and switch to the interaction picture with respect to the Hamiltonian that governs the unitary dynamics. In the rotating-wave approximation, we neglect cross-terms such as  $\hat{d}_1^\dagger \hat{d}_2^\dagger$ , and we thus arrive at the master equation

$$\begin{aligned} \frac{d}{dt} \tilde{\rho}(s, t) = & \kappa \left( \varepsilon_{1-}^2 \mathcal{D}_s[\hat{d}_1] + \varepsilon_{1+}^2 \mathcal{D}_s[\hat{d}_1^\dagger] \right. \\ & \left. + \varepsilon_{2-}^2 \mathcal{D}_s[\hat{d}_2] + \varepsilon_{2+}^2 \mathcal{D}_s[\hat{d}_2^\dagger] + N|r_c|s \right) \tilde{\rho}(s, t), \end{aligned} \quad (35)$$

where  $r_c$  in the superradiant phase is given by Eq. (15), while it vanishes in the normal phase.

The master equation above describes three independent processes. There are the photon emissions from two independent quantum harmonic oscillators as well as the photon emission from a Poisson process with rate  $\kappa N|r_c|$ . As a result, the generating function factorizes as

$$\mathcal{M}_F(s, t) = \mathcal{M}_F^{(1)}(s, t) \mathcal{M}_F^{(2)}(s, t) \mathcal{M}_F^{(p)}(s, t), \quad (36)$$

where  $\mathcal{M}_F^{(1,2)}(s, t)$  are the generating functions corresponding to each of the two harmonic oscillators, while

$$\mathcal{M}_F^{(p)}(s, t) = \exp(\kappa N|r_c|ts) \quad (37)$$

describes the Poissonian emission of photons. In a recent work, some of us determined the generating function of a quantum harmonic oscillator, which reads [52]

$$\mathcal{M}_F^{(j)}(s, t) = \frac{\xi_j^{(2)} e^{\kappa_j t}}{\xi_j^{(2)} \cosh(\xi_j^{(2)} \kappa_j t) + [\xi_j^{(1)}]^2 \sinh(\xi_j^{(2)} \kappa_j t)}, \quad (38)$$

where we have defined the constants

$$\begin{aligned} \kappa_1 &= \kappa \left( \varepsilon_{1-}^2 - \varepsilon_{1+}^2 \right) / 2, \\ \kappa_2 &= \kappa \left( \varepsilon_{2-}^2 - \varepsilon_{2+}^2 \right) / 2, \end{aligned} \quad (39)$$

together with the functions

$$\xi_j^{(k)} = \sqrt{1 - 4\bar{n}_j(1 + \bar{n}_j)[(1+s)^k - 1]} \quad (40)$$

with

$$\begin{aligned} \bar{n}_1 &= \varepsilon_{1+}^2 / (\varepsilon_{1-}^2 - \varepsilon_{1+}^2), \\ \bar{n}_2 &= \varepsilon_{2+}^2 / (\varepsilon_{2-}^2 - \varepsilon_{2+}^2). \end{aligned} \quad (41)$$

These expressions fully characterize the emission statistics of the Dicke model for all possible observation times.

#### IV. LEE-YANG THEORY

We are now ready to use our Lee-Yang theory to detect the superradiant phase transition. In the original theory of equilibrium phase transitions by Lee and Yang, they considered the zeros of the partition function in the complex plane of the control parameters; for instance, an external magnetic field or the inverse temperature [26–29]. For systems of finite size, the zeros are complex and the imaginary part is finite. However, if the system exhibits a phase transition, the zeros will approach the point on the real-axis, where the phase transition occurs, as the system size is increased. The Lee-Yang theory of equilibrium phase transitions has found use across a wide range of fields in physics and related areas [28, 29]. It has also been shown that Lee-Yang zeros can be experimentally determined from the fluctuations of the observable

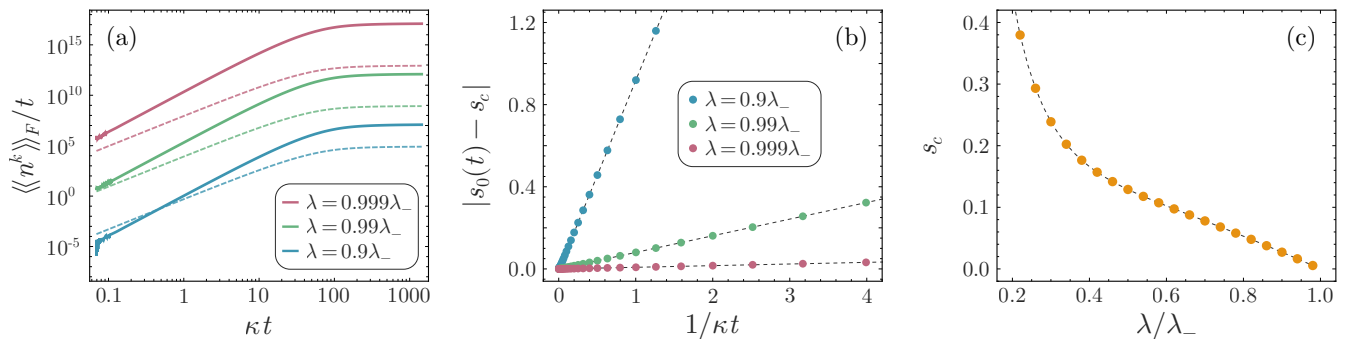


FIG. 2. Lee-Yang theory of the normal phase. (a) Fourth (dashed) and fifth (solid) factorial as a function of the observation time in the normal phase. (b) The dominant pole extracted from the factorial cumulants in panel (a). (c) Convergence point of the dominant pole in the long-time limit as a function of the coupling. Parameters are  $\omega_c = 2\kappa$  and  $\omega_a = 0.5\kappa$ .

that couples to the control parameter [53], for instance, the inverse temperature couples to the energy [54], and a magnetic field may couple to the magnetization of a spin system [55–57]. In addition, Lee-Yang zeros have been determined in several experiments [39–42].

While the theory of Lee and Yang was developed for equilibrium phase transitions [26, 27], it has subsequently been extended to several types of non-equilibrium situations [28–30]. Those include dynamical phase transitions (also known as trajectory phase transitions) [31, 41], dynamical quantum phase transitions in quantum many-body systems after a quench [32–35], as well as to quantum phase transitions at zero temperature [36–38]. In such nonequilibrium situations, the phase transitions are not manifested in the partition function or the associated free-energy density. Instead, other quantities, such as the moment generating function or the Loschmidt amplitude, play the role of the partition function, whose complex zeros determine the phase behavior of the system.

In the approach that we follow here, the generating function in Eq. (23) plays the role of the partition function. The partition function is given by a sum over all possible microconfigurations of an equilibrium system weighted by Boltzmann factors. Similarly, the factorial moment generating function is given by a sum over all possible dynamical trajectories, characterized by the number  $n = 0, 1, 2, \dots$  of photons that have been emitted during the time span  $[0, t]$ , weighted by the counting variable  $s$ . For an equilibrium system, the thermodynamic limit is approached as the system size, for example, the number of spins in a spin lattice, is increased. By contrast, in our case, the thermodynamic limit is approached as the observation time is increased, and the quantum jump trajectories become long. Thus, as our dynamical free-energy density, we take the scaled factorial cumulant generating function, defined in the long-time limit as

$$\Theta_F(s) = \lim_{t \rightarrow \infty} \mathcal{F}_F(s, t)/t = \lim_{t \rightarrow \infty} \ln\{\mathcal{M}_F(s, t)\}/t. \quad (42)$$

In this case, the system exhibits a phase transition, if the dynamical free-energy density becomes nonanalytic at  $s = 0$ . However, the nonanalytic behavior only emerges

in the long-time limit, and one may wonder, if it can be observed in an experiment, where the observation time remains finite. To this end, we note that the nonanalytic behavior of the dynamical free-energy at  $s = 0$  are due to zeros or poles of the factorial moment generating function that approach the origin as the observation time increases. As we will see, these zeros and poles can be determined from measurements of the factorial moments at finite times, and one can determine their converge points in the limit of long observation times by extrapolation.

In general, the factorial moment generating function can have both zeros and poles in the complex plane of the counting variable. For systems of finite size, the partition function only has zeros. However, when dealing with bosons for example, infinitely many states are involved, and the partition function may also have poles [54]. In earlier works, we have developed methods that allow us to extract both the zeros and the poles from the high cumulants [34, 54]. However, for the factorial moment generating function in Eq. (36), the situation simplifies since it only has poles. (At the points, where the numerator vanishes,  $\xi_i^{(2)} = 0$ , the denominator also vanishes, and the function is non-zero.) Thus, in the following, we formally expand the factorial moment generating function in terms of its unknown poles,  $s_q(t)$ , as

$$\mathcal{M}_F(s, t) = e^{sc} \prod_{q=0}^{\infty} [1 - s/s_q(t)]^{-1} \quad (43)$$

where  $c$  is independent of  $s$ . Using the expression for the factorial cumulants in Eq. (27), we then have

$$\langle\langle n^k \rangle\rangle_F(t) = \sum_{q=0}^{\infty} \frac{(k-1)!}{s_q^k(t)}, \quad k > 1. \quad (44)$$

From this expression, we see that the high factorial cumulants are dominated by the pole that is closest to the origin,  $s = 0$ , which allows us to express them as

$$\langle\langle n^k \rangle\rangle_F(t) \simeq \frac{(k-1)!}{s_0^k(t)}, \quad k \gg 1 \quad (45)$$

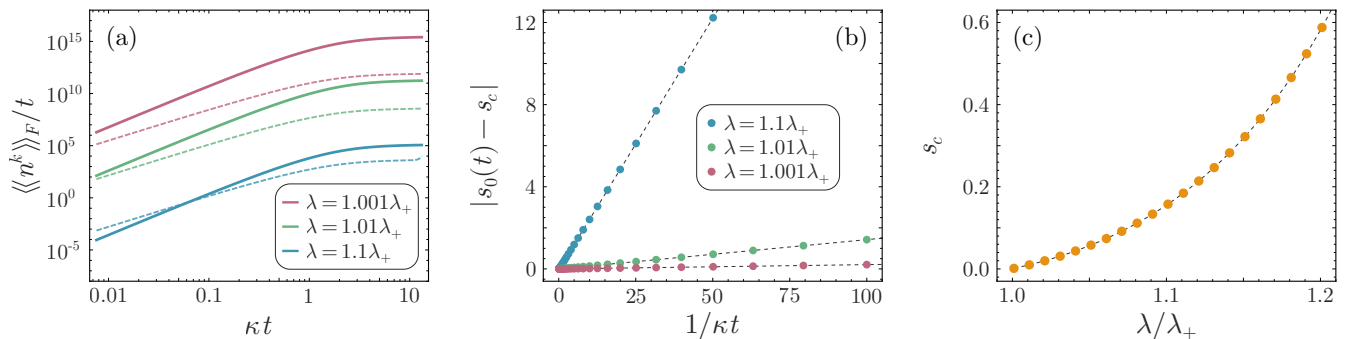


FIG. 3. Lee-Yang theory of the superradiant phase. (a) Fourth (dashed) and fifth (solid) factorial cumulant as a function of the observation time in the superradiant phase. (b) The dominant pole extracted from the results in panel (a). (c) Convergence point in the long-time limit as a function of the coupling. Parameters are  $N = 100$ ,  $\omega_c = 2\kappa$ , and  $\omega_a = 0.5\kappa$ .

for sufficiently high orders. Inverting this expression for the closest pole, we find that it can be expressed as

$$s_0(t) \simeq (k-1) \frac{\langle\langle n^{k-1} \rangle\rangle_F(t)}{\langle\langle n^k \rangle\rangle_F(t)}, \quad k \gg 1 \quad (46)$$

in terms of the high factorial cumulants. Thus, from two high factorial cumulants, which are measurable quantities, we can determine the pole that is closest to the origin, and we can follow its motion as a function of the observation time to determine its convergence point in the thermodynamic limit of long observation times.

## V. PHASE TRANSITIONS

We now extract the pole that is closest to the origin of the complex plane of the counting variable from the high factorial cumulants. This procedure is illustrated in Fig. 2(a), where we show the fourth and fifth factorial cumulants as a function of the observation time for three different couplings in the normal phase. For each coupling, we extract the position of the dominant pole, which we show in Fig. 2(b) as a function of the inverse observation time. The position of the dominant pole is well-approximated by the expression

$$|s_0(t) - s_c| = 1/\kappa t, \quad (47)$$

where  $s_c$  is the convergence point in the limit of long times. Thus, for each value of the coupling, we can extract the convergence point in the long-time limit, and in Fig. 2(c), we show the extracted convergence point as a function of the coupling. For small couplings, the convergence point does not reach the origin. However, as we approach the critical coupling,  $\lambda \simeq \lambda_-$ , the convergence point becomes smaller, and it eventually vanishes at  $\lambda = \lambda_-$ , signaling a phase transition. Thus, from measurements of the fourth and fifth factorial cumulants at finite times, one can detect the phase transition at  $\lambda = \lambda_-$ . In particular, from Figs. 2(a,b), we see that one would be able to determine the convergence point in

the long-time limit from measurements of the factorial cumulants for times that are shorter than  $\kappa t = 1$ .

In Fig. 3, we take the same approach for large couplings, where the system is in the superradiant phase. In Fig. 3(a), we show the fourth and fifth factorial cumulants as a function of the observation time for different couplings. We then show the dominant pole as a function of the inverse observation time, which allows us to extract the convergence points in the long-time limit as shown in Fig. 3(b). In Fig. 3(c), we show the convergence point as a function of the coupling in the superradiant phase. For large couplings,  $\lambda > \lambda_+$ , the convergence point does not reach zero. However, it becomes smaller as the coupling is reduced, and it finally reaches the origin of the complex plane for  $\lambda = \lambda_+$ . Thus, we again see that it is possible to detect the phase transition at  $\lambda = \lambda_+$ , which occurs in the long-time limit, from observations of the high factorial cumulants at finite times.

The results above show how we can detect phase transitions that occur in the limit of long times from measurements of the factorial cumulants during a finite duration. As we now go on to show, the extracted convergence points also influence the large-deviation statistics of the photon emission current. To this end, we invert the expression for the factorial moment generating function in Eq. (23) and write the probability distribution as

$$P(n, t) = \frac{1}{2\pi i} \int_{-i\pi}^{i\pi} ds \mathcal{M}_F(e^s - 1, t) e^{-ns}. \quad (48)$$

Now, defining the photon emission current as  $J = n/t$  and considering the limit of long times, we can write

$$P(J, t) = \frac{1}{2\pi i} \int_{-i\pi}^{i\pi} ds \exp\{[\Theta(s) - sJ]t\}, \quad (49)$$

where we have used that  $\Theta(s) = \Theta_F(e^s - 1)$  is the scaled cumulant generating function. From Eq. (36), we find

$$\Theta(s) = \sum_{j=1}^2 \kappa_j \left( 1 - \sqrt{1 - 4\bar{n}_j(1 + \bar{n}_j)(e^{2s} - 1)} \right) + \kappa N |r_c| (e^s - 1) \quad (50)$$

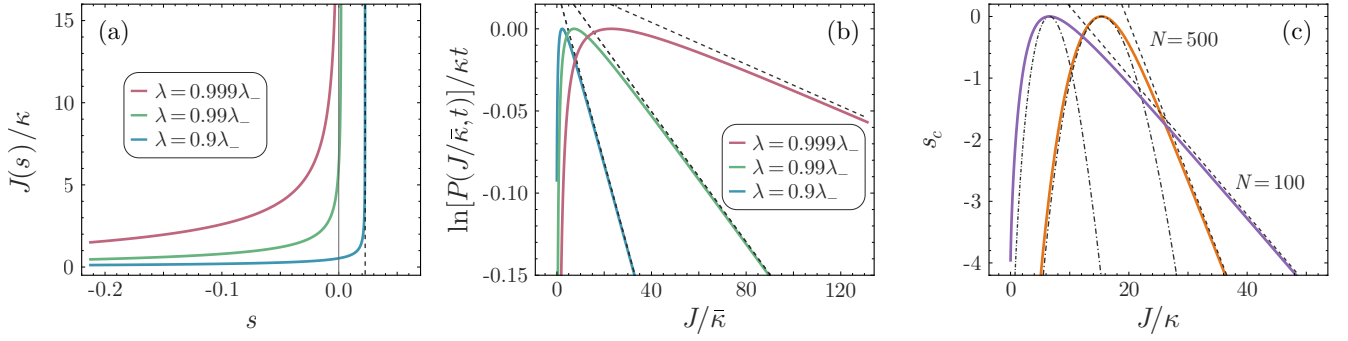


FIG. 4. Large-deviation statistics of the photon emission current. (a) The  $s$ -biased current,  $J(s) = \Theta'(s)$ , in the normal phase given by Eq. (53). (b) Large-deviation statistics in the normal phase given by Eq. (56). The dashed lines are the approximation of the tails based on Eq. (57). (c) Large-deviation statistics in the superradiant phase with  $\lambda = 1.1\lambda_+$  and  $N = 100$  and  $N = 500$ . The other parameters are  $\omega_c = 2\kappa$  and  $\omega_a = 0.5\kappa$ . The dash-dotted lines represent Poisson distributions.

in agreement with Ref. [43]. At long times, the integral in Eq. (49) is amenable to a saddle-point approximation, such that the large-deviation statistics becomes [58]

$$\frac{\ln[P(J, t)]}{t} \simeq \Theta(s_{\text{sp}}) - s_{\text{sp}}J, \quad (51)$$

where  $s_{\text{sp}} = s_{\text{sp}}(J)$  solves the saddle-point equation

$$\Theta'(s_{\text{sp}}) = J. \quad (52)$$

With these definitions at hand, we can calculate the large-deviation statistics of the photon emission current. In the normal phase, we note that  $\bar{n}_1 \gg \bar{n}_2$ , if  $\omega_c \gg \omega_a$  or  $\omega_c \ll \omega_a$ , and the term with  $j = 2$  in Eq. (50) is then negligible. In that case, we find

$$\Theta'(s) = \frac{2e^{2s}\varepsilon_{1+}^2\varepsilon_{1-}^2\kappa/(\varepsilon_{1-}^2 - \varepsilon_{1+}^2)}{\sqrt{1 - (e^{2s} - 1)[2\varepsilon_{1+}\varepsilon_{1-}/(\varepsilon_{1-}^2 - \varepsilon_{1+}^2)]^2}}, \quad (53)$$

$$\frac{\ln[P(J, t)]}{t} \simeq \frac{\varepsilon_{1-}^2 - \varepsilon_{1+}^2}{2}\kappa - \frac{J}{2}\sqrt{\left(\frac{\bar{\kappa}}{J}\right)^2 - 2}\left(\sqrt{1 + \left(\frac{\bar{\kappa}}{J}\right)^2} - 1\right) - \frac{J}{2}\ln\left[\frac{J^2\sqrt{1 + \left(\frac{\bar{\kappa}}{J}\right)^2} - 1}{2\varepsilon_{1+}^2\varepsilon_{1-}^2\kappa^2}\right], \quad (56)$$

which we show in Fig. 4(b) for three different couplings.

To better understand these results, we return to the  $s$ -biased current in Fig. 4(a), where we see that it diverges at the nonanalytic point of the scaled cumulant generating function, and those nonanalytic points are directly related to the convergence points found in Fig. 2(b,c). Thus, for large currents,  $J \gg \bar{\kappa}$ , the saddle-point is given by the convergence point as  $s_{\text{sp}}(J) \simeq e^{s_c} - 1 \simeq s_c$  for  $s_c \ll 1$ , allowing us to approximate the tail of the large-deviation function by the straight line,

$$\frac{\ln[P(J, t)]}{t} \simeq \Theta(s_c) - s_cJ, \quad J \gg \bar{\kappa}, \quad (57)$$

which we show in Fig. 4(b) with dashes. The slope of the

line is given by  $s_c$ , which becomes smaller as the coupling approaches its critical value, and  $s_c$  goes to zero. Thus, we see that the extracted convergence points determine the tails of the large-deviation statistics.

which we will also refer to as the  $s$ -biased current and denote by  $J(s) = \Theta'(s)$ . In Fig. 4(a), we show it for three different couplings in the normal phase.

The solution to the saddle-point equation now becomes

$$s_{\text{sp}} = \frac{1}{2}\ln\left[\frac{J^2\sqrt{1 + \left(\frac{\bar{\kappa}}{J}\right)^2} - 1}{2\varepsilon_{1+}^2\varepsilon_{1-}^2\kappa^2}\right], \quad (54)$$

where we have defined

$$\bar{\kappa} = (\varepsilon_{1+}^2 + \varepsilon_{1-}^2)\kappa. \quad (55)$$

In the normal phase, we then find the expression

The same phenomenon can be observed for the large-deviation statistics in the superradiant phase shown in Fig. 4(c). In that case, we rely on a numerical solution of the saddle-point equation. Still, we again see that the tails of the distribution are determined by the convergence points as shown by dashed lines. Moreover, in the superradiant phase, the bulk of the distribution becomes increasingly Poissonian, as the number of atoms is increased according to Eq. (50). Thus, for the sake of comparison, we show in Fig. 4(c) the large-deviation statistics

line is given by  $s_c$ , which becomes smaller as the coupling approaches its critical value, and  $s_c$  goes to zero. Thus, we see that the extracted convergence points determine the tails of the large-deviation statistics.

The same phenomenon can be observed for the large-deviation statistics in the superradiant phase shown in Fig. 4(c). In that case, we rely on a numerical solution of the saddle-point equation. Still, we again see that the tails of the distribution are determined by the convergence points as shown by dashed lines. Moreover, in the superradiant phase, the bulk of the distribution becomes increasingly Poissonian, as the number of atoms is increased according to Eq. (50). Thus, for the sake of comparison, we show in Fig. 4(c) the large-deviation statistics

for  $N = 100$  and  $N = 500$  atoms together with Poisson distributions that are represented by dotted lines.

## VI. CONCLUSIONS AND OUTLOOK

We have investigated the superradiant phase transition in the open Dicke model using our Lee-Yang theory of phase transitions. Specifically, we have shown how the dominant pole of the factorial cumulant generating function can be extracted from the high factorial cumulants of the photon emission statistics obtained during a finite observation time. As such, our method makes it possible to detect the superradiant phase transition, which occurs in the limit of long times, from measurements of the photon emission statistics, which are limited to finite durations. We have also shown how the convergence point of the dominant pole in the long-time limit determines the tails of the large-deviation statistics. Our method is not restricted to the Dicke model, and it can be applied to other systems that exhibit phase transitions, such as the Rabi model [59–63] or the Lipkin-Meshkov-Glick model [64–67], both in theory and experiments.

We have seen that the system transits directly from the normal phase to the superradiant phase at a specific critical coupling, if the emission rate from the cavity is small. However, for larger decay rates, the critical coupling splits into two different values, and a small gap develops between the two phases. Here, we have applied our Lee-Yang theory to each of the phases, where the system can be mapped onto two uncoupled quantum harmonic oscillators, and the problem can be solved. By contrast, we are not aware of a solution in the gap region, which would allow us to calculate the factorial cumulants and thereby apply our Lee-Yang method. However, we expect that it may be possible to explore this region using a different diagonalization procedure [43], higher-order operator-cumulant expansions beyond the mean-field approximation [4], or advanced numerical methods for systems of finite size. A combination of such approaches might make it possible to explore the region between the two phases using our Lee-Yang formalism. We leave this task as an interesting open problem for future work.

## VII. ACKNOWLEDGMENTS

We acknowledge support from Jane and Aatos Erkko Foundation, Research Council of Finland through the Finnish Centre of Excellence in Quantum Technology (352925), and the Japan Society for the Promotion of Science through an Invitational Fellowship for Research in Japan. F. N. is supported in part by Nippon Telegraph and Telephone Corporation (NTT) Research, the Japan Science and Technology Agency (JST) [via the Quantum Leap Flagship Program (Q-LEAP), and the Moonshot

R&D Grant Number JPMJMS2061], the Asian Office of Aerospace Research and Development (AOARD) (via Grant No. FA2386-20-1-4069), and the Office of Naval Research Global (ONR) (via Grant No. N62909-23-1-2074). N. L. is supported by the RIKEN Incentive Research Program and by MEXT KAKENHI Grant Numbers JP24H00816, JP24H00820.

## Appendix A: Diagonalization parameters

We here provide the parameters for the diagonalization in Eqs. (9) and (10). To this end, we introduce the dimensionless parameters,  $\tilde{\omega}_{1,2} = \omega_{1,2}/\omega_c$ , with similar meanings for other parameters with a tilde.

In the normal phase, we have

$$\varepsilon_{1\pm} = \sin(\gamma) \frac{1 \mp \tilde{\omega}_1}{2\sqrt{\tilde{\omega}_1}}, \quad \varepsilon_{2\pm} = \cos(\gamma) \frac{1 \mp \tilde{\omega}_2}{2\sqrt{\tilde{\omega}_2}}, \quad (\text{A1})$$

with

$$\tilde{\omega}_1 = \sqrt{\left(1 + \tilde{\omega}_a^2 \pm \sqrt{(\tilde{\omega}_a^2 - 1)^2 + 16\tilde{\lambda}^2\tilde{\omega}_a}\right)}/2, \quad (\text{A2})$$

and

$$\tilde{\omega}_2 = \sqrt{\left(1 + \tilde{\omega}_a^2 \mp \sqrt{(\tilde{\omega}_a^2 - 1)^2 + 16\tilde{\lambda}^2\tilde{\omega}_a}\right)}/2, \quad (\text{A3})$$

where the signs are plus for  $\tilde{\omega}_a > 1$  and minus for  $\tilde{\omega}_a \leq 1$ . Furthermore, the parameter  $\gamma$  is obtained from

$$\tan(2\gamma) = 4\tilde{\lambda} \frac{\sqrt{\tilde{\omega}_a}}{\tilde{\omega}_a^2 - 1}. \quad (\text{A4})$$

For the superradiant phase, the eigenfrequencies are

$$\tilde{\omega}_1 = \sqrt{\left(1 + 4\tilde{\lambda}_{\text{aa}}\tilde{\Omega}_a + \tilde{\Omega}_a^2 \pm \sqrt{\alpha}\right)}/2, \quad (\text{A5})$$

and

$$\tilde{\omega}_2 = \sqrt{\left(1 + 4\tilde{\lambda}_{\text{aa}}\tilde{\Omega}_a + \tilde{\Omega}_a^2 \mp \sqrt{\alpha}\right)}/2, \quad (\text{A6})$$

where the signs are determined in the same way as for the normal phase. We have also introduced the parameter

$$\alpha = 1 + 8\left(2\tilde{\lambda}_{\text{ca}}^2 - \tilde{\lambda}_{\text{aa}}\right)\tilde{\Omega}_a - 2\left(1 - 8\tilde{\lambda}_{\text{aa}}^2\right)\tilde{\Omega}_a^2 + 8\tilde{\lambda}_{\text{aa}}\tilde{\Omega}_a^3 + \tilde{\Omega}_a^4, \quad (\text{A7})$$

and the parameter  $\gamma$  is obtained from

$$\cos(\gamma) = \sqrt{\frac{\tilde{\Omega}_a^2}{2\sqrt{\alpha}} + \frac{2}{\sqrt{\alpha}}\tilde{\lambda}_{\text{aa}}\tilde{\Omega}_a - \frac{1}{2}\left(1 + \frac{1}{\sqrt{\alpha}}\right)}. \quad (\text{A8})$$



- 
- [1] R. H. Dicke, Coherence in Spontaneous Radiation Processes, *Phys. Rev.* **93**, 99 (1954).
- [2] K. Hepp and E. H. Lieb, On the superradiant phase transition for molecules in a quantized radiation field: the Dicke maser model, *Ann. Phys.* **76**, 360 (1973).
- [3] Y. K. Wang and F. T. Hioe, Phase Transition in the Dicke Model of Superradiance, *Phys. Rev. A* **7**, 831 (1973).
- [4] P. Kirton, M. M. Roses, J. Keeling, and E. G. Dalla Torre, Introduction to the Dicke Model: From Equilibrium to Nonequilibrium, and Vice Versa, *Adv. Quant. Technol.* **2**, 1970013 (2018).
- [5] N. Lambert, Y.-N. Chen, R. Johansson, and F. Nori, Quantum chaos and critical behavior on a chip, *Phys. Rev. B* **80**, 165308 (2009).
- [6] P. Nataf and C. Ciuti, No-go theorem for superradiant quantum phase transitions in cavity QED and counterexample in circuit QED, *Nat. Commun.* **1**, 72 (2010).
- [7] O. Viehmann, J. von Delft, and F. Marquardt, Superradiant Phase Transitions and the Standard Description of Circuit QED, *Phys. Rev. Lett.* **107**, 113602 (2011).
- [8] T.-L. Wang, L.-N. Wu, W. Yang, G.-R. Jin, N. Lambert, and F. Nori, Quantum Fisher information as a signature of the superradiant quantum phase transition, *New J. Phys.* **16**, 063039 (2014).
- [9] N. Lambert, Y. Matsuzaki, K. Kakuyanagi, N. Ishida, S. Saito, and F. Nori, Superradiance with an ensemble of superconducting flux qubits, *Phys. Rev. B* **94**, 224510 (2016).
- [10] M. Bamba, K. Inomata, and Y. Nakamura, Superradiant Phase Transition in a Superconducting Circuit in Thermal Equilibrium, *Phys. Rev. Lett.* **117**, 173601 (2016).
- [11] F. Minganti, I. I. Arhipov, A. Miranowicz, and F. Nori, Continuous dissipative phase transitions with or without symmetry breaking, *New J. Phys.* **23**, 122001 (2021).
- [12] D. De Bernardis, P. Pilar, T. Jaako, S. De Liberato, and P. Rabl, Breakdown of gauge invariance in ultrastrong-coupling cavity QED, *Phys. Rev. A* **98**, 053819 (2018).
- [13] O. Di Stefano, A. Settineri, V. Macrì, L. Garziano, R. Stassi, S. Savasta, and F. Nori, Resolution of gauge ambiguities in ultrastrong-coupling cavity quantum electrodynamics, *Nat. Phys.* **15**, 803 (2019).
- [14] S. Ashhab, Y. Matsuzaki, K. Kakuyanagi, S. Saito, F. Yoshihara, T. Fuse, and K. Semba, Spectrum of the Dicke model in a superconducting qubit-oscillator system, *Phys. Rev. A* **99**, 063822 (2019).
- [15] S. Genway, W. Li, C. Ates, B. P. Lanyon, and I. Lesanovsky, Generalized Dicke Nonequilibrium Dynamics in Trapped Ions, *Phys. Rev. Lett.* **112**, 023603 (2014).
- [16] S. De Liberato and C. Ciuti, Quantum Phases of a Multimode Bosonic Field Coupled to Flat Electronic Bands, *Phys. Rev. Lett.* **110**, 133603 (2013).
- [17] C. Emary and T. Brandes, Quantum Chaos Triggered by Precursors of a Quantum Phase Transition: The Dicke Model, *Phys. Rev. Lett.* **90**, 044101 (2003).
- [18] C. Emary and T. Brandes, Chaos and the quantum phase transition in the Dicke model, *Phys. Rev. E* **67**, 066203 (2003).
- [19] N. Lambert, C. Emary, and T. Brandes, Entanglement and the Phase Transition in Single-Mode Superradiance, *Phys. Rev. Lett.* **92**, 073602 (2004).
- [20] F. Dimer, B. Estienne, A. S. Parkins, and H. J. Carmichael, Proposed realization of the Dicke-model quantum phase transition in an optical cavity QED system, *Phys. Rev. A* **75**, 013804 (2007).
- [21] Z. Zhiqiang, C. H. Lee, R. Kumar, K. J. Arnold, S. J. Masson, A. S. Parkins, and M. D. Barrett, Nonequilibrium phase transition in a spin-1 Dicke model, *Optica* **4**, 424 (2017).
- [22] K. Baumann, C. Guerlin, F. Brennecke, and T. Esslinger, Dicke quantum phase transition with a superfluid gas in an optical cavity, *Nature* **464**, 1301 (2010).
- [23] D. Nagy, G. Kónya, G. Szirmai, and P. Domokos, Dicke-Model Phase Transition in the Quantum Motion of a Bose-Einstein Condensate in an Optical Cavity, *Phys. Rev. Lett.* **104**, 130401 (2010).
- [24] E. G. D. Torre, S. Diehl, M. D. Lukin, S. Sachdev, and P. Strack, Keldysh approach for nonequilibrium phase transitions in quantum optics: Beyond the Dicke model in optical cavities, *Phys. Rev. A* **87**, 023831 (2013).
- [25] Y.-H. Chen, Y. Qiu, A. Miranowicz, N. Lambert, W. Qin, R. Stassi, Y. Xia, S.-B. Zheng, and F. Nori, Sudden change of the photon output field marks phase transitions in the quantum Rabi model, *Commun. Phys.* **7**, 5 (2024).
- [26] C. N. Yang and T. D. Lee, Statistical Theory of Equations of State and Phase Transitions. I. Theory of Condensation, *Phys. Rev.* **87**, 404 (1952).
- [27] T. D. Lee and C. N. Yang, Statistical Theory of Equations of State and Phase Transitions. II. Lattice Gas and Ising Model, *Phys. Rev.* **87**, 410 (1952).
- [28] R. A. Blythe and M. R. Evans, The Lee-Yang theory of equilibrium and nonequilibrium phase transitions, *Braz. J. Phys.* **33**, 464 (2003).
- [29] I. Bena, M. Droz, and A. Lipowski, Statistical mechanics of equilibrium and nonequilibrium phase transitions: The Yang-Lee formalism, *Int. J. Mod. Phys. B* **19**, 4269 (2005).
- [30] R. A. Blythe and M. R. Evans, Lee-Yang Zeros and Phase Transitions in Nonequilibrium Steady States, *Phys. Rev. Lett.* **89**, 080601 (2002).
- [31] C. Flindt and J. P. Garrahan, Trajectory Phase Transitions, Lee-Yang Zeros, and High-Order Cumulants in Full Counting Statistics, *Phys. Rev. Lett.* **110**, 050601 (2013).
- [32] M. Heyl, A. Polkovnikov, and S. Kehrein, Dynamical Quantum Phase Transitions in the Transverse-Field Ising Model, *Phys. Rev. Lett.* **110**, 135704 (2013).
- [33] K. Xu, Z.-H. Sun, W. Liu, Y.-R. Zhang, H. Li, H. Dong, W. Ren, P. Zhang, F. Nori, D. Zheng, H. Fan, and H. Wang, Probing dynamical phase transitions with a superconducting quantum simulator, *Sci. Adv.* **6**, eaba4935 (2020).
- [34] S. Peotta, F. Brange, A. Deger, T. Ojanen, and C. Flindt, Determination of Dynamical Quantum Phase Transitions in Strongly Correlated Many-Body Systems Using Loschmidt Cumulants, *Phys. Rev. X* **11**, 041018 (2021).
- [35] F. Brange, S. Peotta, C. Flindt, and T. Ojanen, Dynamical quantum phase transitions in strongly correlated two-dimensional spin lattices following a quench, *Phys. Rev. Res.* **4**, 033032 (2022).
- [36] T. Kist, J. L. Lado, and C. Flindt, Lee-Yang theory of

- criticality in interacting quantum many-body systems, *Phys. Rev. Res.* **3**, 033206 (2021).
- [37] P. M. Vecsei, J. L. Lado, and C. Flindt, Lee-Yang theory of the two-dimensional quantum Ising model, *Phys. Rev. B* **106**, 054402 (2022).
- [38] P. M. Vecsei, C. Flindt, and J. L. Lado, Lee-Yang theory of quantum phase transitions with neural network quantum states, *Phys. Rev. Res.* **5**, 033116 (2023).
- [39] C. Binek, Density of Zeros on the Lee-Yang Circle Obtained from Magnetization Data of a Two-Dimensional Ising Ferromagnet, *Phys. Rev. Lett.* **81**, 5644 (1998).
- [40] X. Peng, H. Zhou, B.-B. Wei, J. Cui, J. Du, and R.-B. Liu, Experimental Observation of Lee-Yang Zeros, *Phys. Rev. Lett.* **114**, 010601 (2015).
- [41] K. Brandner, V. F. Maisi, J. P. Pekola, J. P. Garrahan, and C. Flindt, Experimental Determination of Dynamical Lee-Yang Zeros, *Phys. Rev. Lett.* **118**, 180601 (2017).
- [42] H. Gao, K. Wang, L. Xiao, M. Nakagawa, N. Matsumoto, D. Qu, H. Lin, M. Ueda, and P. Xue, Experimental Observation of the Yang-Lee Quantum Criticality in Open Quantum Systems, *Phys. Rev. Lett.* **132**, 176601 (2024).
- [43] W. Kopylov, C. Emary, and T. Brandes, Counting statistics of the Dicke superradiance phase transition, *Phys. Rev. A* **87**, 043840 (2013).
- [44] T. Holstein and H. Primakoff, Field dependence of the intrinsic domain magnetization of a ferromagnet, *Phys. Rev.* **58**, 1098 (1940).
- [45] D. V. Kapor, M. J. Škrinjar, and S. D. Stojanović, Relation between spin-coherent states and boson-coherent states in the theory of magnetism, *Phys. Rev. B* **44**, 2227 (1991).
- [46] D. Kambly, C. Flindt, and M. Büttiker, Factorial cumulants reveal interactions in counting statistics, *Phys. Rev. B* **83**, 075432 (2011).
- [47] D. Kambly and C. Flindt, Time-dependent factorial cumulants in interacting nano-scale systems, *J. Comp. Elec.* **12**, 331 (2013).
- [48] P. Stegmann, B. Sothmann, A. Hucht, and J. König, Detection of interactions via generalized factorial cumulants in systems in and out of equilibrium, *Phys. Rev. B* **92**, 155413 (2015).
- [49] J. König and A. Hucht, Newton series expansion of bosonic operator functions, *SciPost Phys.* **10**, 007 (2021).
- [50] E. Kleinherbers, P. Stegmann, A. Kurzman, M. Geller, A. Lorke, and J. König, Pushing the Limits in Real-Time Measurements of Quantum Dynamics, *Phys. Rev. Lett.* **128**, 087701 (2022).
- [51] M. B. Plenio and P. L. Knight, The quantum-jump approach to dissipative dynamics in quantum optics, *Rev. Mod. Phys.* **70**, 101 (1998).
- [52] F. Brange, P. Menczel, and C. Flindt, Photon counting statistics of a microwave cavity, *Phys. Rev. B* **99**, 085418 (2019).
- [53] A. Deger, K. Brandner, and C. Flindt, Lee-Yang zeros and large-deviation statistics of a molecular zipper, *Phys. Rev. E* **97**, 012115 (2018).
- [54] F. Brange, T. Pyhäranta, E. Heinonen, K. Brandner, and C. Flindt, Lee-Yang theory of Bose-Einstein condensation, *Phys. Rev. A* **107**, 033324 (2023).
- [55] B.-B. Wei and R.-B. Liu, Lee-Yang Zeros and Critical Times in Decoherence of a Probe Spin Coupled to a Bath, *Phys. Rev. Lett.* **109**, 185701 (2012).
- [56] B.-B. Wei, S.-W. Chen, H.-C. Po, and R.-B. Liu, Phase transitions in the complex plane of physical parameters, *Sci. Rep.* **4**, 5202 (2014).
- [57] A. Deger, F. Brange, and C. Flindt, Lee-Yang theory, high cumulants, and large-deviation statistics of the magnetization in the Ising model, *Phys. Rev. B* **102**, 174418 (2020).
- [58] H. Touchette, The large deviation approach to statistical mechanics, *Phys. Rep.* **478**, 1 (2009).
- [59] S. Ashhab, Superradiance transition in a system with a single qubit and a single oscillator, *Phys. Rev. A* **87**, 013826 (2013).
- [60] M.-J. Hwang, R. Puebla, and M. B. Plenio, Quantum Phase Transition and Universal Dynamics in the Rabi Model, *Phys. Rev. Lett.* **115**, 180404 (2015).
- [61] M.-J. Hwang, P. Rabl, and M. B. Plenio, Dissipative phase transition in the open quantum Rabi model, *Phys. Rev. A* **97**, 013825 (2018).
- [62] R.-H. Zheng, W. Ning, Y.-H. Chen, J.-H. Lü, L.-T. Shen, K. Xu, Y.-R. Zhang, D. Xu, H. Li, Y. Xia, F. Wu, Z.-B. Yang, A. Miranowicz, N. Lambert, D. Zheng, H. Fan, F. Nori, and S.-B. Zheng, Observation of a Superradiant Phase Transition with Emergent Cat States, *Phys. Rev. Lett.* **131**, 113601 (2023).
- [63] Z.-Y. Ge, H. Fan, and F. Nori, Effective field theories and finite-temperature properties of zero-dimensional superradiant quantum phase transitions, *Phys. Rev. Res.* **6**, 023123 (2024).
- [64] H. J. Lipkin, N. Meshkov, and A. J. Glick, Validity of many-body approximation methods for a solvable model, *Nucl. Phys.* **62**, 188 (1965).
- [65] N. Meshkov, A. J. Glick, and H. Lipkin, Validity of many-body approximation methods for a solvable model, *Nucl. Phys.* **62**, 199 (1965).
- [66] A. J. Glick, H. J. Lipkin, and N. Meshkov, Validity of many-body approximation methods for a solvable model, *Nucl. Phys.* **62**, 211 (1965).
- [67] W. Kopylov, G. Schaller, and T. Brandes, Nonadiabatic dynamics of the excited states for the Lipkin-Meshkov-Glick model, *Phys. Rev. E* **96**, 012153 (2017).